An MD Simulation of Concentrated Aqueous Solutions of Caesium Iodide

Y. Tamura and H. Ohtaki

Coordination Chemistry Laboratories, Institute for Molecular Science, Myodaiji-cho, Okazaki, 444 Japan

I. Okada

Department of Electronic Chemistry, Tokyo Institute of Technology at Nagatsuta, Nagatsuta-cho, Midori-ku, Yokohama, 227 Japan

Z. Naturforsch. **46a,** 1083–1094 (1991); received April 12, 1991

Molecular dynamics simulations of concentrated aqueous CsI solutions have been performed for $CsI:H_2O = 1:20$ (2.78 molal) at 298 K and 341 K and 1:10 (5.56 molal) at 349 K. Effects of temperature and concentration on the structures of the hydrated ions, the ion pairs, and ionic aggregates are discussed by comparing the results with X-ray diffraction data obtained under similar conditions [1].

I. Introduction

In a previous paper [1] we have reported the result of an X-ray diffraction study on concentrated aqueous solutions of CsI and LiI with various concentrations at room and elevated temperatures and discussed the effect of temperature and concentration on the hydration structure of the ions. For the CsI solutions it was found that about 80% of the ions form ion pairs in the 2.78 molal solution at 293 K and that the degree of ion-pair formation exceeds 100% in the 5.56 molal solution at 343 K. The result suggested that ionic aggregates such as $[Cs_2I]^+$, $[CsI_2]^-$, or even higher ones, should be formed especially in a highly concentrated solution. However, it was not possible to determine the structure of the aggregates from the analyses of the radial distribution functions (RDFs), because the peak appearing at about 700 pm in the RDFs, in which structural information on the aggregates should be involved, was broad and not well separated from other peaks in the curve.

In early molecular dynamics (MD) simulations of aqueous CsF [2, 3], CsCl [2] and LiI [4] solutions and of water microclusters containing a single ion such as Na^+, Rb^+, Cs^+, F^-, Br^-, and I^- [5], empirical potential functions were adopted for the ion-water interactions, which consisted of a Lennard-Jones term for short-range interactions and a Coulomb term involving four point charges on a water molecule and an elementary at the centre of the ion.

A number of MD simulations of alkali and alkaline earth halides in water have been performed so far [6–11], and recently lanthanum(III) chloride solutions were included [12]. The potential functions between water molecules and metal or halide ions have been estimated by ab initio calculations. Studies of systems containing large and soft ions have thus not been examined due to enormously increasing difficulties in the ab initio calculations. Interaction energies of an iodide ion and a water molecule have been calculated for several configurations around the minimum only [13], and no MD simulation of aqueous CsI solutions has been reported so far.

In this paper we shall discuss the temperature and concentration dependence of the hydration structure of ions, ion pairs, and aggregates which have been suggested to exist by the X-ray diffraction measurement [1].

II. Pair Potential Functions

A) Water-Water Potential

Many models of intermolecular interaction potentials between water molecules have been proposed and explored in simulations. They can be classified into two categories; the rigid models, including ST2 [14], MCY and its modifications [15], and the flexible

Reprint requests to Prof. H. Ohtaki, Coordination Chemistry Laboratories, Institute for Molecular Science, Myodaiji-cho, Okazaki, 444 Japan.

0932-0784 / 91 / 1200-1083 $ 01.30/0. – Please order a reprint rather than making your own copy.

models as exemplified by the central force [16] and the Watts' models [17]. The central force model of water has been modified to become a flexible three-site model [18] consisting of intra- and intermolecular parts in order to evaluate the frequency shift of the internal vibrations on the transition from the gas phase to the liquid state. However, in order to save computation time, we adopted the original central force model of water [16]. The discrepancy between the original central force and the flexible three-site model is very small as far as the intermolecular interaction is concerned.

B) Ion-Water Potential

Simulations of aqueous solutions containing caesium or iodide ions have been performed so far for CsF [2, 3], CsCl [2], and LiI [4] aqueous solutions using the ST2 model. As Cs^+- and I^--water potentials compatible with the central force model for water have not been reported, they were derived here in the following way: Firstly, the interaction energies between an ion modelled as a charged Lennard-Jones sphere [19] and an ST2-modelled water molecule were calculated for four typical configurations: (i) the negative pole of the water dipole pointing towards the ion, (ii) the positive pole of the water dipole pointing towards the ion, (iii) a proton in a water molecule pointing towards the ion, (iv) a negative charge in the ST2 model pointing towards the ion. The calculated values for Cs^+-water and I^--water interactions are shown as the solid lines in Figs. 1 a and 1 b, respectively. Secondly, in order to obtain the site-site potentials for the central force model, the ion-O and ion-H potentials were assumed as

$$V_{\mathrm{Iw}}(r) = \frac{Z_{\mathrm{I}} Z_{\mathrm{w}}}{4\pi\varepsilon_0 r} + \frac{A_{\mathrm{Iw}}}{r^2} + B_{\mathrm{Iw}} \exp[-C_{\mathrm{Iw}} r], \qquad (1)$$

where I and w denote the ion and an interaction site of a water molecule, respectively, and the parameter values, A_{Iw}, B_{Iw}, and C_{Iw}, were optimized to fit to the energies obtained from the ST2-model calculations. Z_{I} is the formal charge of Cs^+ or I^-, and Z_{w} is the charge on a site of a water molecule in the central force model, $Z_{\mathrm{H}} = 0.32983\,e$ and $Z_{\mathrm{O}} = -2\,Z_{\mathrm{H}}$. The O–H distance and the H–O–H bond angle were fixed at 95.72 pm and 104.5°, respectively. The most stable configuration, namely (i) for the Cs^+-water (Fig. 1 a) and (ii) for the I^--water (Fig. 1 b), were weighted in the fitting procedure so that the minimum energies and their positions should give a reasonable agreement with the calculated curves with the ST2 model. The obtained potentials are shown as the dashed lines in Figs. 1 a and 1 b.

After preliminary runs extended over several thousand steps, it was found that the peaks for the Cs–O and Cs–I bonds appeared at slightly larger distances than those obtained by the X-ray diffraction measurements [1]. Therefore, the parameter values in the third term on the right-hand side of (1) for the Cs-water interactions, and the size parameter, σ_{CsCs} in (2), were reduced to some extent by a trial and error method until the best fit was obtained between the experimental and calculated peak positions in the RDFs. The final parameter values thus evaluated are listed in Table 1. Figure 1 a shows a comparison among Cs-water interaction energies calculated by using the ST2 model (solid lines), the curves fitted to the solid lines by using the central force model (dashed lines), and the curves evaluated by the CF model with the values modified to obtain the best fit to the RDFs (dotted lines).

C) Ion-Ion Potentials

Several ion-ion pair potentials for CsI are found in the literature; a Born-Mayer-Huggins type function used in a Monte Carlo simulation of molten salts [20], a Woodcock potential used for a series of alkali halide crystals [21], and a function of the charged Lennard-Jones type used for a series of MD simulations for alkali halides in water [2–4, 19], etc. The potential functions of the last example consist of a point charge at the centre of atom and a soft core of the Lennard-Jones type:

$$V_{ij}(r) = \frac{Z_i Z_j}{4\pi\varepsilon_0 r} + 4\varepsilon_{ij}\left\{\left(\frac{\sigma_{ij}}{r}\right)^2 + \left(\frac{\sigma_{ij}}{r}\right)^6\right\}, \qquad (2)$$

where Z_i and Z_j are the formal charges on ions. ε_{ij} and σ_{ij} are the Lennard-Jones parameters. The parameters for the Cs–I pair were calculated by using Kong's combination rule [22]. Since the size parameter for the

Table 1. Parameters for the ion-water potentials.

	Cs–O	Cs–H	I–O	I–H
$A_{\mathrm{Iw}}/10\,\mathrm{J\,m^2}$	−2.1297	−0.13779	−4.1561	0.86868
$B_{\mathrm{Iw}}/10^{-13}\,\mathrm{J}$	0.38292	2.07888	1.89501	0.12229
$C_{\mathrm{Iw}}/10^{10}\,\mathrm{m^{-1}}$	5.076	5.3066	5.672	4.8256

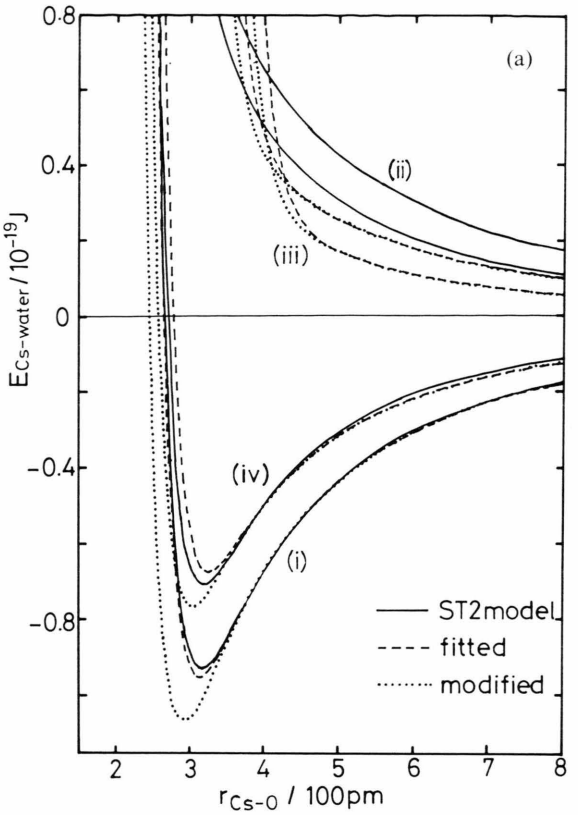

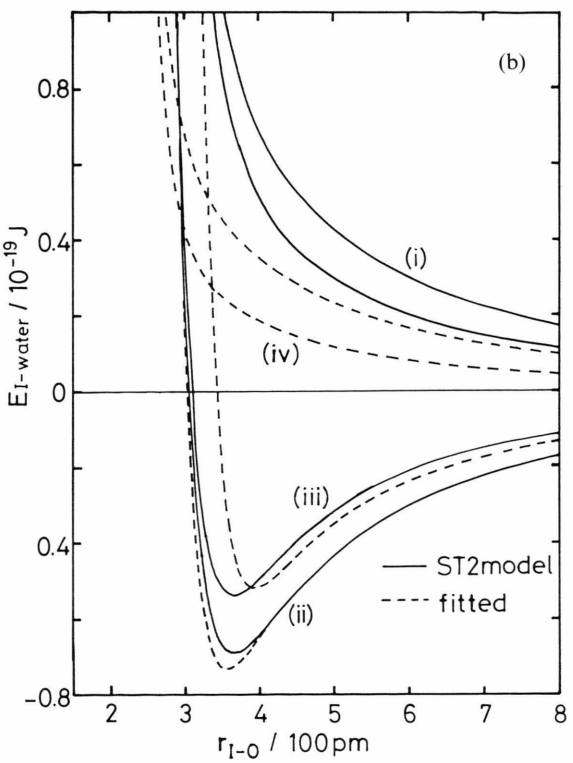

Fig. 1. Fitted and modified ion-water potentials for the four configurations (I)–(IV) mentioned in the text. Solid line: ST2 model and Lennard-Jones type potential; dashed line: fitted; dots: modified. (a) Caesium-water, (b) iodide-water.

Table 2. Lennard-Jones parameters for the ion-ion potentials.

	Cs–Cs	I–I	Cs–I
$\varepsilon_{ij}/10^{-23}$ J	354.0	67.8	134.6
$\sigma_{ij}/10^{-10}$ m	3.42	5.40	4.40

Table 3. The number of particles n and the side length of a basic cube L. T_0, and T_{av} denote the initial and the average temperatures, respectively.

	n_O	n_H	n_{Cs}	n_I	L/pm	T_0/K	T_{av}/K
(A)	200	400	10	10	1913	293	298
(B)	200	400	10	10	1927	343	341
(C)	180	360	18	18	1944	343	349

Cs ion, σ_{CsCs}, was slightly changed from the original value in the literature [19], the parameters for the Cs–I interaction were also changed. The results are given in Table 2.

III. Procedures of the Simulations

In order to compare the RDFs obtained from the present MD simulations with those from the X-ray diffraction experiments, the MD simulations were carried out under conditions similar to the ones in the X-ray diffraction studies [1]. Table 3 shows the number of particles n, the side length of the basic cell L, and the average temperature during the simulations. According to [23], the solubility of CsI is 3.0 molal ($CsI:H_2O = 1:18.3$) at 293 K and 6.6 molal (1:8.4) at 343 K under atmospheric pressure. The side length of the basic cell was calculated from the measured density [1]. The integration time step was 0.5 fs. After equilibrium had been achieved, the simulation was continued without correcting the temperature. The last 12,000 steps, which correspond to 6 ps, were used for the evaluation of $g(r)$'s and other properties. The Ewald summation was employed for the Coulomb interactions. The equation of motion was solved by a modified Verlet algorithm.

Since the number of both caesium and iodide ions is much smaller than that of water molecules and,

moreover, the ions have large masses compared to that of a water molecule, the initial configuration of ions in the basic cell should significantly affect the succeeding configurations of ions and molecules during the calculation. In order to avoid such an influence we first assumed the masses of all particles, including H and O atoms, to be unity to accelerate the motions. After the system reached an equilibrium, the atomic weights of the particles were changed to those given in the periodic table. This procedure saved much CPU time. Several thousand steps were needed after changing the masses of the particles in order to achieve equilibrium.

IV. Results and Discussion

A) Radial Distribution Functions (RDFs)

The pair correlation function for the i-j pair is calculated from the histogram of N_{ij} for intervals $(r, r+\Delta r)$,

$$g_{ij}(r) = \frac{V}{4\pi N_i N_j r^2} \left\langle \frac{N_{ij}(r, r+\Delta r)}{\Delta r} \right\rangle, \tag{3}$$

where N_i is the number of the i-th kind of particles in the volume V of the basic cell. N_j is the number of the j-th kind for unlike pairs, which is equal to $(N_i - 1)/2$ for like pairs by definition. The hydration number can be estimated from the running integration number $n_{ij}(r)$, which is defined as

$$n_{ij}(r) = \frac{4\pi N_j}{V} \int_0^r r^2 g_{ij}(r)\, \mathrm{d}r. \tag{4}$$

If $n_{ij}(r)$ does not display a plateau over a certain range of r, the definition of the hydration number is not unique. n_{ij} at the first minimum of $g(r)$ is frequently adopted in order to compare the hydration numbers of ions evaluated from simulations with those obtained from X-ray and neutron diffraction experiments [24]. In this paper we use the following definitions for the cases that the first peak is not well separated from others: (a) twice the value of n_{ij} at the position of the first maximum, r_M, in $g_{ij}(r)$ obtained from the simulation, $(2n_{ij}(r_M))$, (b) n_{ij} at the distance r_2 where $g_{ij}(r)$ becomes unity after the first maximum, $(n_{ij}(r_2))$, and (c) n_{ij} at the first minimum r_m, $(n_{ij}(r_m))$.

Table 4. Comparison of the first peaks and the number of interactions obtained by X-ray diffraction [1] and the present MD simulations. The number of interactions is given as $n(r_2)$, definition (C), see text.

	r_{CsO}/ pm	n_{CsO}	r_{IO}/ pm	n_{IO}	r_{CsI}/ pm	n_{CsI}	Ref.
(A) MD	303	5.78	364	12.7	387	1.07	present work
X-ray	301	5.75	367	7.2	388	0.80	[1]
(B) MD	303	5.26	369	12.5	390	0.83	present work
X-ray	306	4.73	360	8.2	385	0.81	[1]
(C) MD	305	6.04	365	12.2	381	1.80	present work
X-ray	302	3.04	372	6.8	385	1.18	[1]

1. Comparison with X-Ray Data

The structure function, $s \cdot i(s)$, is obtained from the weighted sum of the functions $(g_{ij}(r) - 1)$;

$$s \cdot i(s) = \frac{\sum_i \sum_j x_i x_j f_i(s) f_j(s)}{\{\sum x_i f_i(s)\}^2} \cdot \int_0^{r_{max}} 4\pi r \varrho \{g_{ij}(r) - 1\} \sin(sr)\, \mathrm{d}r, \tag{5}$$

where s is the scattering variable ($s = 4\pi\lambda^{-1} \sin\Theta$, where Θ is one half of the scattering angle at λ, the wavelength of the X-ray). x_i and $f_i(s)$ denote the mole fraction and the X-ray scattering factor for the i-th kind of scattering centres, respectively. ϱ is the mean number density of the system. By taking the Fourier transform, the X-ray weighted radial distribution function $G^x(r)$, is obtained:

$$G^x(r) - 1 = \frac{1}{2\pi^2 \varrho r} \int_0^{s_{max}} s \cdot i(s) \sin(sr)\, \mathrm{d}s, \tag{6}$$

where s_{max} is a maximum value achieved in the measurement.

In Fig. 2 the calculated $G^x(r)$'s are compared with the ones obtained from the X-ray diffraction experiments [1]. Table 4 summarizes the distances between ions and water molecules and between ions, together with the numbers of interactions as defined by $n_{ij}(r_2)$. Since the size parameter for the caesium ion was modified in order to reproduce the experimental values, the calculated Cs–O and Cs–I distances agree with the observed ones within about 1% for all solutions. The I–O distance coincides with the observed one within about 2%. Although the peak positions are well reproduced by the MD simulations, the peaks in the simulated $G^x(r)$'s are much sharper than those obtained by the X-ray study.

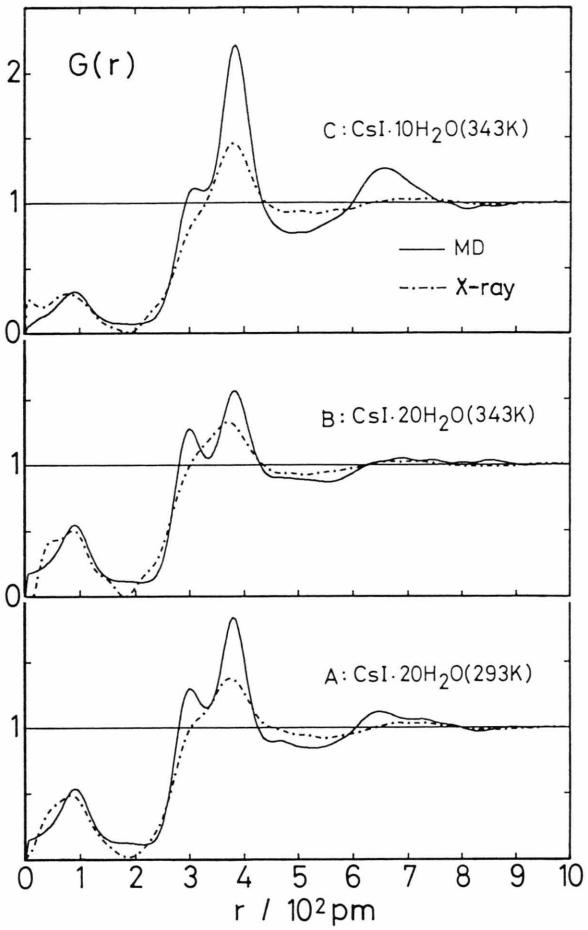

Fig. 2. Comparison of the X-ray weighted radial distribution functions from the simulation solid with experimental data (dot dashed).

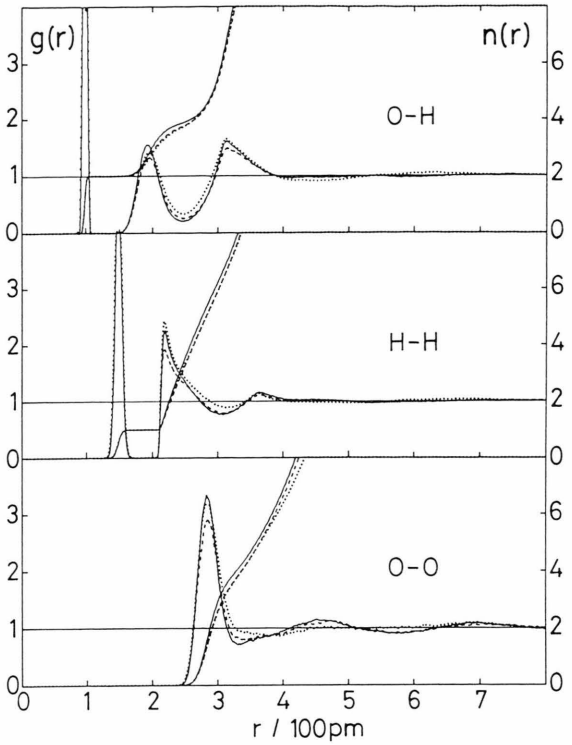

Fig. 3. Water-water pair correlation functions and running integration numbers for the solutions A (solid line), B (dashed line), and C (dotted line).

2. Water-Water Pair Correlation Function

Figure 3 shows the pair correlation functions, $g(r)$, and the running integration numbers, $n(r)$, for the water-water interactions in the three solutions. The intramolecular interactions appear as sharp peaks at 96 pm in g_{OH} and at 150 pm in g_{HH}. The peak positions for the first neighbours are almost the same for all the solutions. An increase in temperature causes broadening of the first neighbour peaks. With increasing concentration the modulation of g_{OO} above 320 pm is reduced, suggesting that the distribution beyond the first neighbour shell becomes more random. It should be noted that the height of the peak at 285 pm in g_{OO} increases with increasing concentration of the solute, while the running integration number remains practically unchanged up to 320 pm.

3. Hydration of the Cation

The peak position for Cs–O at 304 pm is practically independent of both temperature and concentration, as seen in Figure 4. The Cs–O distance is 18 pm shorter than that estimated in CsF solutions [2, 3]. The shortening arises from the fact that the parameter of the caesium ion was changed so as to fit the X-ray data. The number of Cs–O interactions decreases with increasing temperature (solution A to B) and increases with increasing concentration (solution B to C). However, the concentration effect found in the experiment was opposite, as seen in Table 4. The temperature dependence of the Cs–H peak position is less clear. With increasing concentration the peak shifts to shorter distances, this is accompanied by an increase in the number of contact ion pairs. Penetration of iodide ions into the first hydration shell of the caesium

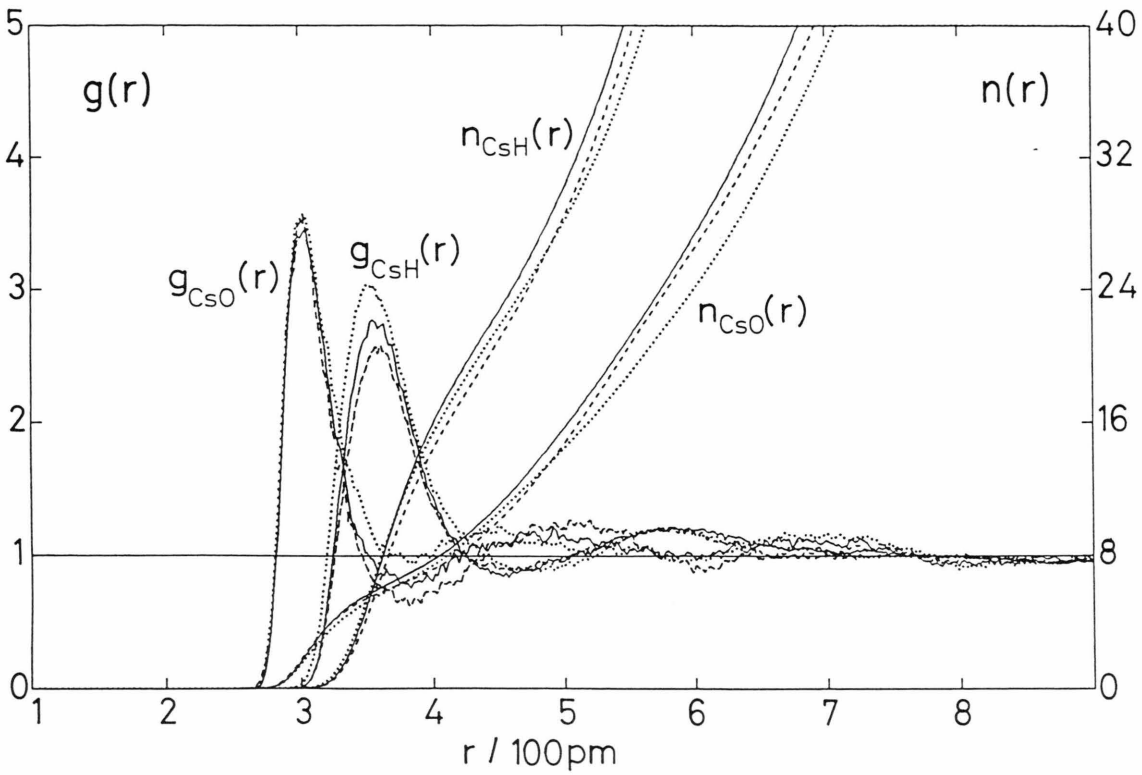

Fig. 4. Caesium-oxygen and caesium-hydrogen pair correlation functions and running integration numbers for the solutions A (solid line), B (dashed line), and C (dotted line).

ion should result in a change of orientation of the water molecules.

In spite of the fact that the first peak is not well separated, a loose second hydration shell seems to cause the broad peaks in the region 420 to 550 pm at low concentrations (solutions A and B). With an increase in concentration the depth of the first minimum approaches unity, and the modulation beyond the first peak becomes ambiguous.

4. Hydration of the Anion

As seen in Fig. 5, the first peaks in the $g_{IO}(r)$ and $g_{IH}(r)$ functions are more diffuse than those in the corresponding functions of the cation. In a comparison of the hydration numbers estimated from the MD simulation with those from the X-ray measurements, $2n_{IO}(r_M)$ yields the best agreement among the three values (see Tables 4 and 5).

With increasing temperature the position of the first I–O peak is slightly shifted towards larger distances, and the hydration number decreases. The peak position shifts towards shorter distances. The hydration number decreases slightly with increasing concentration, which is understandable in terms of an increase in the ion-pair formation. The first peak in the $g_{IH}(r)$ function shows the same trend as that in the $g_{IO}(r)$ function. Since the hydration number calculated from the area of the first peak of $g_{IH}(r)$ is close to that of the $g_{IO}(r)$ curve, water molecules in the first coordination shell orient in the way that one hydration atom points towards the iodide ion. This result agrees with that form an LiI solution [4].

5. Ion-Ion Pair Correlation Function

Ion-ion pair correlation functions are depicted with their running integration numbers in Fig. 6, and the peak data are listed in Table 6.

The Cs–I interaction appears for all solutions as a sharp peak located at about 385 pm, the bond distance corresponding to the sum of the effective ionic

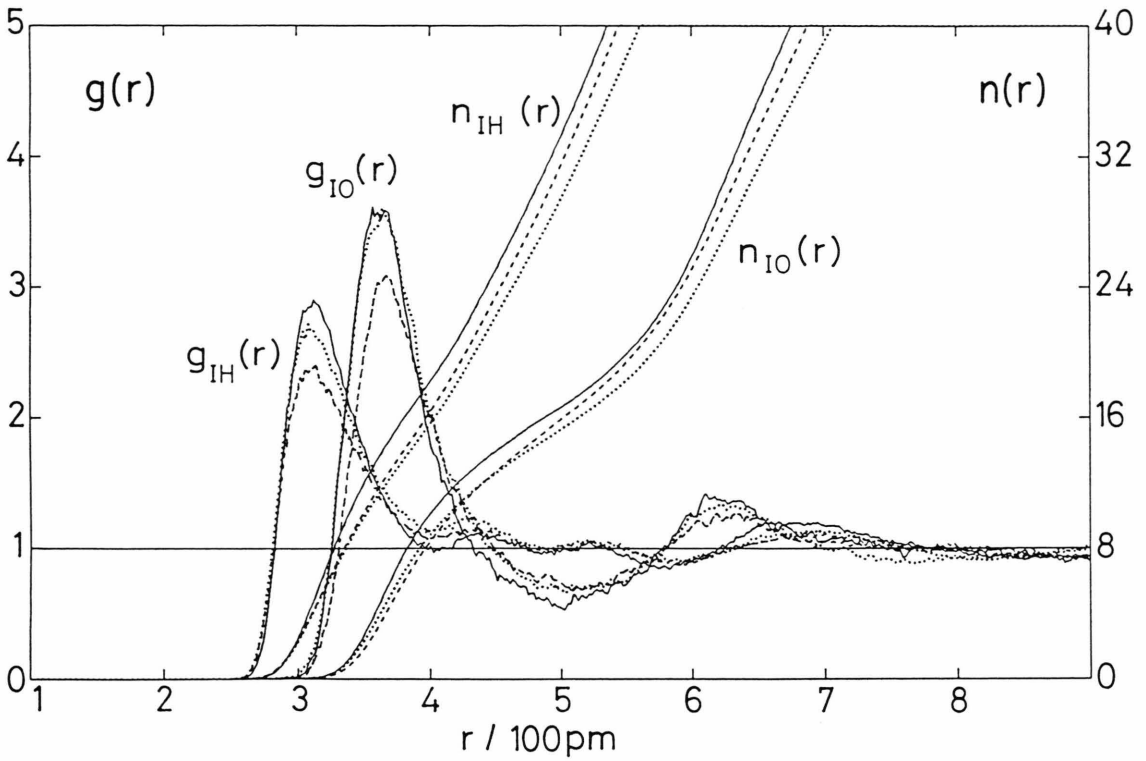

Fig. 5. Iodide-oxygen and iodide-hydrogen pair correlation functions and running integration numbers for the solutions A (solid line), B (dashed line), and C (dotted line).

radii. The peak broadens and the number of interactions is reduced at the higher temperature (solution B); the second peak at about 640 pm shiftes toward larger distances and also broadenes significantly. The small peaks in $g_{CsCs}(r)$ and $g_{II}(r)$ at about 500 pm and 550 pm, respectively, vanish completely. The fact that the number of Cs–I interactions exceedes unity at 298 K suggests the formation of aggregates in solution A. As the solubility of caesium iodide in water increases with increasing temperature in the real system, the slight disintegration of the aggregates with increasing temperature seems to be reasonable, although the trend was not obvious from the X-ray diffraction measurement.

With increasing concentration the coordination number of the Cs–I interactions increases up to about 2, and the second peak at about 630 pm appears again. A prepeak around 540 pm appears in $g_{CsCs}(r)$, and in $g_{II}(r)$ the emergence of the first peak shifts towards shorter distances. This means that more aggregates are formed in solution C than in solution B. If it is taken into account that solutions A and C are nearly saturated, the formation of such aggregates can be regarded as an emergence of nuclei for crystallization. The structure of the aggregates will be discussed later.

B) Distribution of Hydration Numbers and Angular Correlation Functions

As the angular distribution function $P(\cos\theta)$ is a function of the number of neighbours, which depends on the distance, we used r_2 as cutoff distance. The results obtained were similar to those where the minimum distances, r_m, was used for the cutoff.

1. Distribution of Hydration Numbers and Angular Distribution of the First Neighbours

The histograms in Fig. 7 show the frequencies of various nearest water molecules arrangements for the

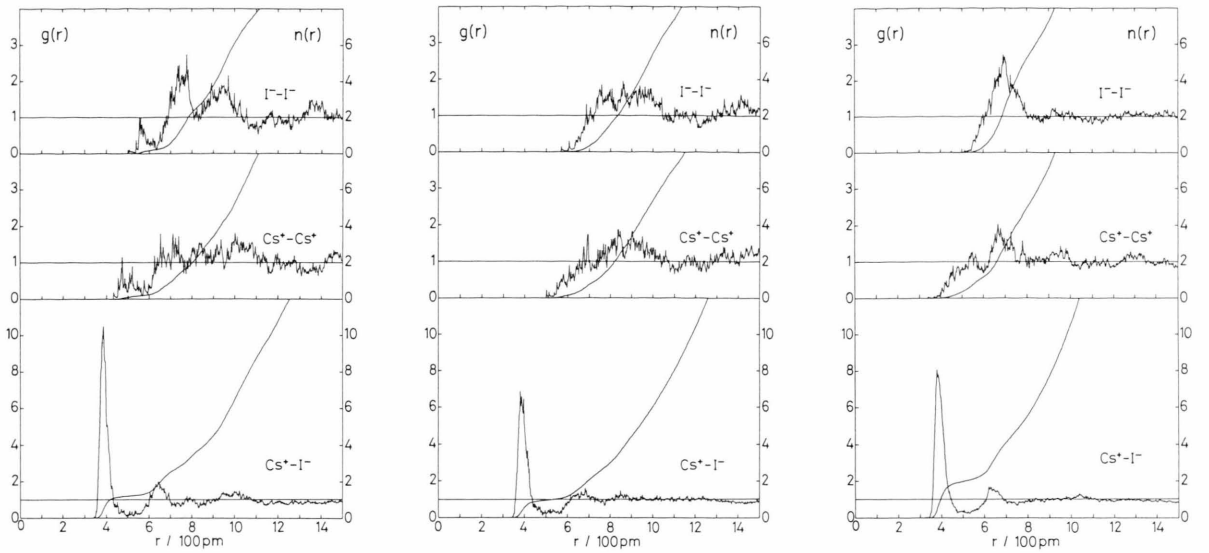

Fig. 6. Ion-ion pair correlation functions and running integration numbers from left to right; (A) 2.78 molal at 298 K, (B) 2.78 molal at 341 K, and (C) 5.56 molal at 349 K.

Table 5. Characteristic values r_M, r_2, and r_m^* in the ion-water pair correlation functions and their corresponding running integration numbers $n(r)$.

			(A)		(B)		(C)	
Cs–O	r_M		303		303		305	
		$2n(r_M)$		4.0		4.2		4.0
	r_2		355		347		370	
		$n(r_2)$		5.78		5.26		6.04
	r_m		385		383		385	
		$n(r_m)$		7.03		6.50		6.65
Cs–H	r_M		359		361		352	
		$2n(r_M)$		14.3		13.5		11.6
	r_2		425		424		442	
		$n(r_2)$		19.4		17.6		20.7
	r_m		452		456		480	
		$n(r_m)$		22.8		21.6		25.0
I–O	r_M		364		369		365	
		$2n(r_M)$		9.8		8.6		8.6
	r_2		433		449		445	
		$n(r_2)$		12.7		12.5		12.2
	r_m		503		510		510	
		$n(r_m)$		16.7		16.4		15.7
I–H	r_M		314		311		310	
		$2n(r_M)$		10.3		8.0		7.5
	r_2		—		—		—	
		$n(r_2)$		—		—		—
	r_m		416		408		404	
		$n(r_m)$		19.9		17.1		15.9

* Distances are given in pm.

Table 6. Characteristic values r_M, r_2, and r_m^* in the Cs–I pair correlation functions and their corresponding running integration numbers $n(r)$.

		(A)		(B)		(C)	
r_M		387		390		381	
r_2		433		440		446	
	$n(r_2)$		1.07		0.83		1.80
r_m		≈510		≈520		≈510	
	$n(r_m)$		1.2		0.97		2.0

* Distances are given in pm.

caesium and iodide ions. At the lower temperature and concentration (solution A), the hydration number 6 is the most probable value for caesium ion, this maximum shifts to 5 at the higher temperature (solution B). The increase in temperature causes an increase in the effective repulsion between the neighbouring water molecules due to the acceleration of translational and rotational motions. At the high concentration (solution C), the maximum of 6 is recovered again. This is an unexpected finding, because the number of contact ion pairs increases and the iodide ion should exclude some of hydrated water molecules. This can, however, be interpreted in terms of most of neighbouring water molecules being shared between the iodide and the caesium ion.

Angular correlation functions of water molecules for various hydration number around the caesium ions are depicted in Figure 8. In the solutions A and B, a broad peak located at about 70° and a small peak at about 50° increase their heights with increasing hydration number. In solution C, the latter peak be-

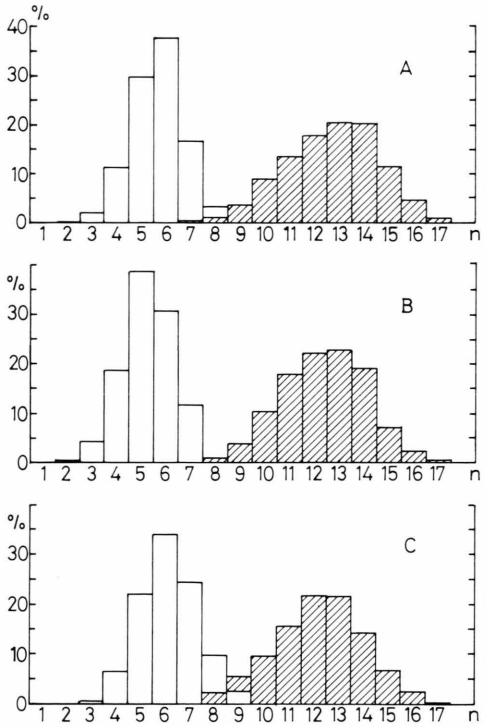

Fig. 7. Probability histograms of the number of nearest neighbour water molecules within a cutoff distance of r_2 for the solutions A, B, and C. Open and hatched columns indicate caesium and iodide ions, respectively.

comes dominant with increasing hydration number, while the former peak flattens at CN = 8. The broad peaks appearing at about 70° can be assigned to the correlations of the water molecules that are not influenced by an iodide ion. The peaks at about 50° correspond to the angle where the coordinated water molecules contact tightly with each other. As it tends to increase in height with increasing concentration, the penetration of iodide ions into the first hydration shell of the caesium ion might affect this peak. Compared with the hydrated lithium ion [25], where a fairly strong angular correlation was observed, the water molecules around the caesium ion are distributed rather randomly.

In the case of the iodide ion, the distribution of hydration numbers spreads widely from 7 to 17 in all solutions, as seen in Figure 7. The maximum appears between 13 and 14 at the lower temperature and concentration (solution A). With increasing temperature (solution B), the distribution moves toward smaller numbers and the maximum shifts to between 12 and 13. The reason for the temperature dependence can be explained in a similar manner as for the caesium ion discussed above. In contrast to the case of the caesium ion, the distribution shows a small shift toward smaller numbers with increasing concentration, but the maximum is still between 12 and 13 (solution C).

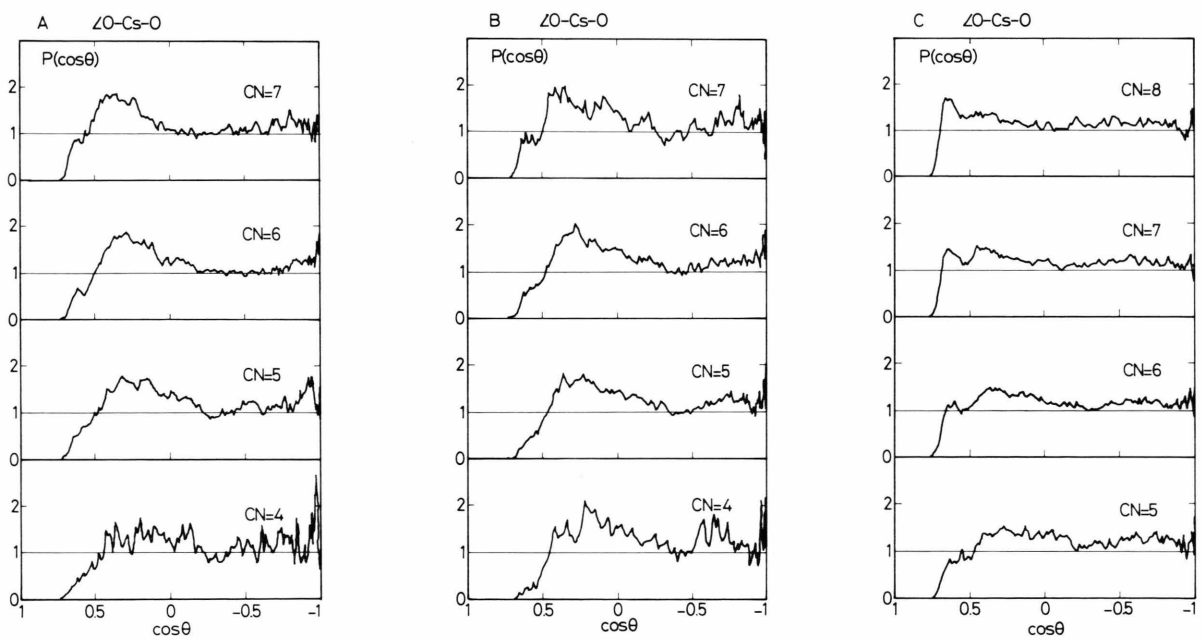

Fig. 8. Correlation of the angle O–Cs–O with coordination numbers CN for the solutions A, B, and C.

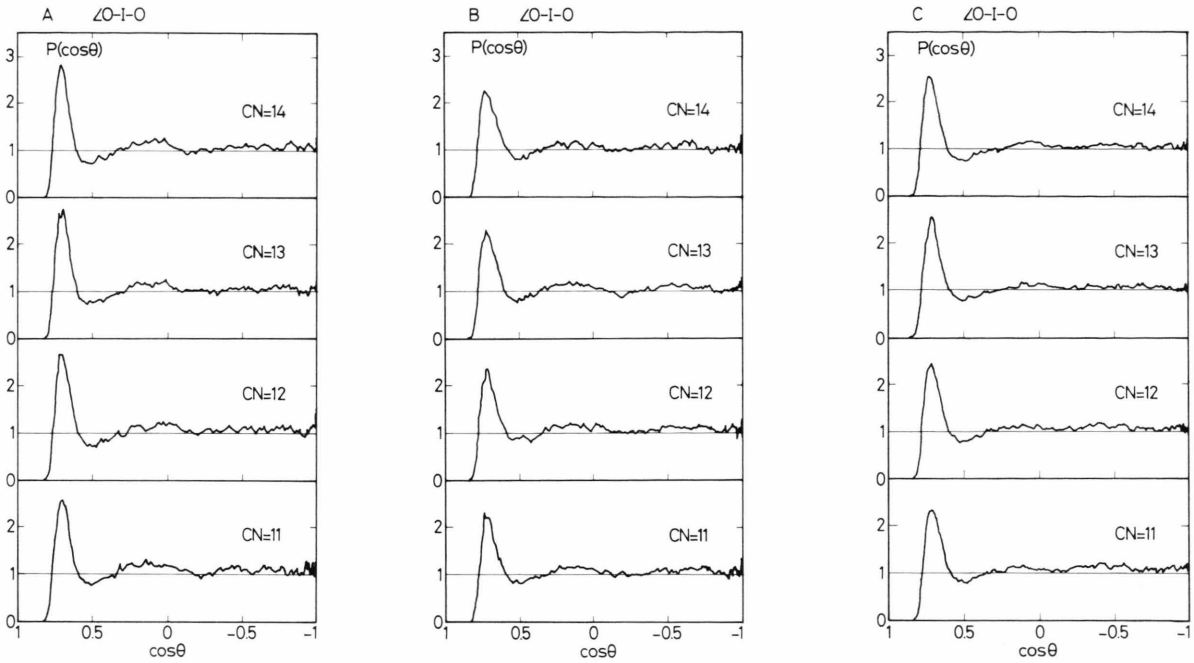

Fig. 9. Correlation of the angle O–I–O with coordination numbers CN for the solutions A, B, and C.

The angular correlation functions for the anion hydration shells are shown in Fig. 9 for four different coordination numbers. The general shape is very similar for all solutions and hydration numbers. A rather sharp peak appears at about 45°; beyond this first peak there is no appreciable correlation, although a broad peak can be seen around 80°. The angle 45° corresponds to the correlation between contact water molecules hydrating the iodide ion. The angular correlation for the hydrated chloride ion in a lithium chloride solution [25] shows very similar features, notwithstanding the fact that the interaction between a chloride ion and water molecules is much stronger than that between an iodide ion and water molecules. The large hydration numbers and the wide range of the distributions found for both anions may be a reason for this similarity.

2. Angular Correlations of the First Neighbour Ion-Ion Interactions

The distributions of the number of nearest neighbour ion-ion interactions are delineated with respect to the iodide ions around a caesium ion, and vice versa, in Figure 10. Here the cutoff distances are set at r_2. At the low concentrations (solutions A and B),

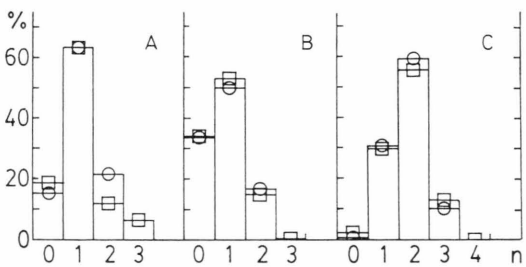

Fig. 10. Probability histograms of the number of counterions within the cutoff distance of r_2, for the solutions A, B, and C. Squares and circles indicate caesium ions around an iodide ion, and iodide ions around a caesium ion, respectively.

more than half of the ions form 1:1 contact pairs. The fraction of free ions increases about twofold with increasing temperature; the result shows that a certain amount of ion pairs and aggregates decomposes. This trend agrees with the temperature dependence of the solubility of CsI. Interestingly, higher order aggregates in solution A contain some iodide ions that have three neighbouring caesium ions, while none of the caesium ions has three iodide ions in its neighbourhood. This suggests that aggregates Cs_3I exist in solution A. At the high concentration (solution C), the

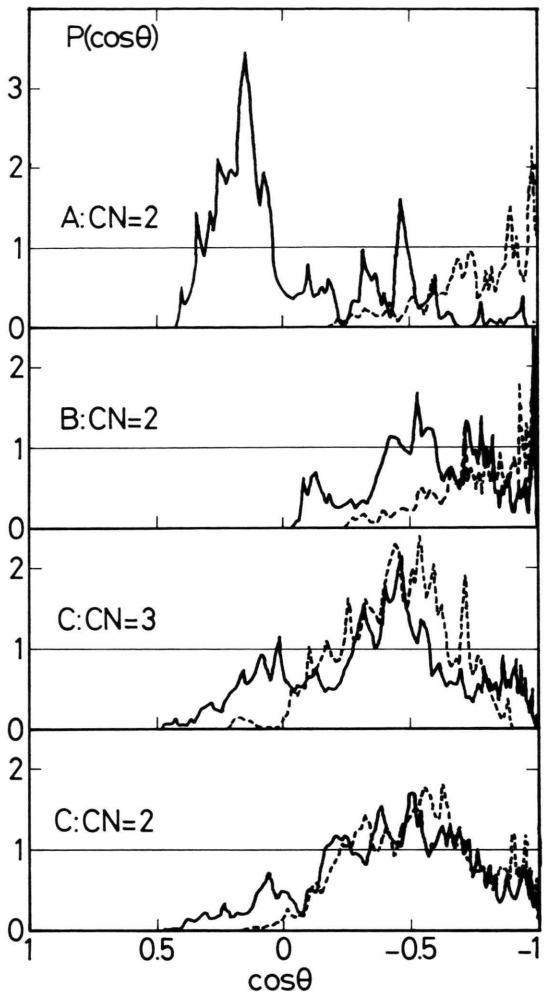

Fig. 11. Correlation of the angles Cs–I–Cs (solid line) and I–Cs–I (broken line) for the solutions A, B, and C.

concentration of the higher order aggregates increases and that of the free ions decreases drastically. As solution C is an almost saturated one, this variation can be expected.

The angular correlation functions around the caesium and iodide ions are depicted in Figure 11. The correlations between iodide ions around a caesium ion show practically no temperature dependence (solutions A and B in Figure 11). The distribution tends to increase towards 180°, where the conformation I–Cs–I is linear. On the contrary, the correlations of caesium ions around an iodide ion change drastically at low temperature (solution A in Fig. 11) and a large peak appears at about 80°. A second peak is seen at about 120°. With increase in temperature the peak at 80° disappears completely and the correlations above 120° increase. The angular correlation function for $[Cs_3I]$ is highly scattered due to the low statistics, and is therefore not shown here.

The angular distribution is strongly concentration dependent. At high concentration (solution C in Fig. 11) the angular correlation function of iodide ions around a caesium ion shows a broad peak at about 120° in the cases of coordination numbers of two and three. This is not found at low concentrations (solutions A and B). The angular distribution function of caesium ions around an iodide ion shows a large peak at about 120° and a small peak at about 85° (solution C in Figure 12). Although the ratio of the peak heights is reversed, they can be compared to the peaks appearing at the low temperature and concentration (solution A). This might be interpreted in terms of the decomposition of the aggregates formed in solution A at the elevated temperature but the decomposition was suppressed with the increase in the concentration.

V. Concluding Remarks

Several diffraction experiments containing either caesium or iodide ions in water are reported in the literature. X-ray diffraction data for the Cs–O distance are found in the region from 301 to 315 pm [1, 26, 27], while a neutron diffraction study yielded a shorter distance of 295 pm [28]. The I–O distances determined by X-ray diffraction range from 355 to 376 pm [1]. This variance of the bond distances seems to be too large in view of the experimental errors. Not only the hydration numbers but also the bond distances might thus depends on the concentration if the number of water molecules is not enough to fill up the hydration shells.

In the present work, the temperature and concentration dependence of ionic aggregations has been discussed on the basis of the pair and angular distribution functions. At the highest concentration and temperature the coordination number of the Cs–I interaction is about two. The angular distribution function of iodide ions around a caesium ion has a maximum at about 120°, and that of caesium ions around an iodide ion has a large peak at about 120° and a small peak at about 85°. The latter becomes the main peak at low temperature and concentration. In an fcc struc-

ture, the angular distribution function of the first neighbours shows two peaks at 90° and 180°. For caesium halide crystals, except for CsF which has the bcc structure, the angular distribution function should have maxima at 70.5°, 109.5°, and 180°. Since the angular distribution function of solution A has peaks around 80° and 120°, as well as 180°, bcc-like aggregates may be formed in the solution. Moreover, since the coordination numbers of the caesium and iodide ions are two at the high concentration, aggregates Cs_2I_2 seem to be formed in solution C, which can be regarded as nuclei of caesium iodide crystals.

[1] Y. Tamura, T. Yamaguchi, I. Okada, and H. Ohtaki, Z. Naturforsch. **42a,** 367 (1987).
[2] K. Heinzinger and P. C. Vogel, Z. Naturforsch. **31a,** 463 (1976).
[3] Gy. I. Szász and K. Heinzinger, Z. Naturforsch. **38a,** 214 (1983).
[4] Gy. I. Szász, K. Heinzinger, and W. O. Riede, Z. Naturforsch. **36a,** 1067 (1981); Gy. I. Szász and K. Heinzinger, Earth and Planetary Science Letters **64,** 163 (1983).
[5] C. L. Briant and J. J. Burton, J. Chem. Phys. **60**, 2849 (1973); **64,** 2888 (1976).
[6] K. Tanaka, N. Ogita, Y. Tamura, I. Okada, H. Ohtaki, G. Pálinkás, E. Spohr, and K. Heinzinger, Z. Naturforsch. **42 a,** 24 (1987); Y. Tamura, K. Tanaka, E. Spohr, and K. Heinzinger, Z. Naturforsch. **43a,** 1103 (1988).
[7] P. Bopp, W. Dietz, and K. Heinzinger, Z. Naturforsch. **34a,** 1424 (1979).
[8] T. Yamaguchi, H. Ohtaki, E. Spohr, G. Pálinkás, K. Heinzinger and M. M. Probst, Z. Naturforsch. **41a,** 1175 (1986); M. M. Probst, E. Spohr, and K. Heinzinger, Chem. Phys. Lett. **161,** 405 (1989).
[9] W. Dietz, W. O. Riede, and K. Heinzinger, Z. Naturforsch. **37a,** 1038 (1982).
[10] G. Pálinkás, T. Radnai, W. Dietz, Gy. I. Szász, K. Heinzinger, Z. Naturforsch. **37a,** 1049 (1982).
[11] E. Spohr, G. Pálinkás, K. Heinzinger, P. Bopp, and M. M. Probst, J. Phys. Chem. **92,** 6754 (1988).
[12] W. Meier, P. Bopp, M. M. Probst, E. Spohr, and J.-L. Lin, J. Phys. Chem. **94,** 4672 (1990).
[13] B. M. Rode, Z. Naturforsch. **31a,** 1081 (1976).
[14] F. H. Stillinger and A. Rahman, J. Chem. Phys. **60**, 1545 (1974).
[15] O. Matsuoka, E. Clementi, and M. Yoshimine, J. Chem. Phys. **64,** 1351 (1976); V. Carravetta and E. Clementi, J. Chem. Phys. **81,** 2646 (1984).
[16] H. L. Lemberg and F. H. Stillinger, J. Chem. Phys. **62,** 1677 (1975); A. Rahman, F. H. Stillinger, and H. L. Lemberg, J. Chem. Phys. **63,** 5223 (1975); F. H. Stillinger and A. Rahman, J. Chem. Phys. **68,** 666 (1978).
[17] R. O. Watts, Chem. Phys. **26,** 367 (1977).
[18] P. Bopp, G. Jancsó, and K. Heinzinger, Chem. Phys. Lett. **98,** 129 (1983).
[19] G. Pálinkás, W. O. Riede, and K. Heinzinger, Z. Naturforsch. **32a,** 1137 (1977).
[20] C. Margheritis, Gazz. Chim. Itali **106,** 309 (1976).
[21] L. V. Woodcock, J. Chem. Soc. Faraday Trans. 2, **70,** 1405 (1974); J. D. Pandy and R. P. Pandy, J. Chem. Soc. Faraday Trans. 2, **77,** 419 (1981).
[22] C. L. Kong, J. Chem. Phys. **59,** 2464 (1973).
[23] W. F. Linke (A. Seidell), Solubilities of Inorganic and Metal-Organic Compounds, 4th Ed., D. Van Nostrand, Amsterdam, Vol. I, 1958.
[24] P. Bopp, K. Heinzinger, and G. Jancsó, Z. Naturforsch. **32a,** 620 (1977).
[25] P. Bopp, I. Okada, H. Ohtaki, and K. Heinzinger, Z. Naturforsch. **40a,** 116 (1985).
[26] R. M. Lawrence and R. F. Kruh, J. Chem. Phys. **47,** 4758 (1967).
[27] H. Bertagnolli, J.-U. Weidner, and H. W. Zimmermann, Ber. Bunsen. Phys. Chem. **78,** 2 (1974).
[28] N. Ohtomo and K. Arakawa, Bull. Chem. Soc. Japan **52,** 2755 (1979).